Journal of Medicinal Chemistry

ARTICLE

pubs.acs.org/jmc

Refining the Eosinophil Cationic Protein Antibacterial Pharmacophore by Rational Structure Minimization

Marc Torrent,[†,‡] David Pulido,[†] Beatriz G. de la Torre,[‡] M. Flor García-Mayoral,[§] M. Victòria Nogués,[†] Marta Bruix,[§] David Andreu,[*,‡] and Ester Boix[*,†]

[†]Department of Biochemistry and Molecular Biology, Universitat Autònoma de Barcelona, E-08193 Cerdanyola del Vallès, Spain

[‡]Department of Experimental and Health Sciences, Pompeu Fabra University, Barcelona Biomedical Research Park, Dr. Aiguader, 88, E-08003 Barcelona, Spain

[§]Rocasolano Institute of Physical Chemistry, CSIC, Serrano 119, 28006 Madrid, Spain

Supporting Information

ABSTRACT: Sequence analysis of eosinophil cationic protein (ECP), a ribonuclease of broad antimicrobial activity, allowed identification of residues 1−45 as the antimicrobial domain. We have further dissected ECP(1−45) with a view to defining the minimal requirements for antimicrobial activity. Structure-based downsizing has focused on both α-helices of ECP(1−45) and yielded analogues with substantial potency against Gram-negative and -positive strains. Analogues ECP(8−36) and ECP(6−17)-Ahx-(23−36) (Ahx, 6-aminohexanoic acid) involve 36% and 40% size reduction relative to (1−45), respectively, and display a remarkably ECP-like antimicrobial profile. Both retain segments required for self-aggregation and lipolysaccharide binding, as well as the bacterial agglutination ability of parent ECP. Analogue (6−17)-Ahx-(23−36), in particular, is shown by NMR to preserve the helical traits of the native 8−16 (α1) and 33−36 (α2) regions and can be proposed as the minimal structure capable of reproducing the activity of the entire protein.

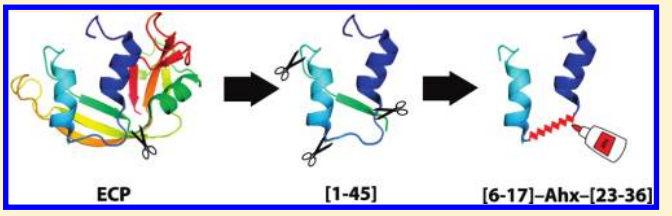

INTRODUCTION

An alarming increase in bacterial resistance to classical antibiotics has become a serious concern among health professionals and spurred intense efforts toward the development of new antimicrobial leads. In this context, antimicrobial peptides (AMPs) are viewed as promising candidates because of their substantial potency, broad spectrum, and distinct mechanism of action.[1] AMPs target bacterial membranes to which they are driven by mainly electrostatic interactions and which upon binding they disrupt, collapsing transmembrane gradients and eventually causing cell death.[2] Bacterial strategies for resisting AMPs require substantial membrane (phospholipid and protein) remodeling, a demanding task that explains the very low incidence of AMP resistance in bacteria.[3]

A number of AMPs are fragments of larger proteins, either naturally derived by proteolysis (e.g., the cathelicidins[4]) or derived by peptide synthesis approaches.[5] In the latter case, educated deconstruction of complex antimicrobial proteins has allowed the identification of structural features essential for bioactivity.[6,7] Although this pharmacophore dissection process is not straightforward and still requires a substantial amount of trial-and-error, it is worthwhile in that defining such minimal structural motifs provides helpful clues for developing therapeutically useful AMP templates.[8]

Eosinophil cationic protein (ECP, RNase 3) is a secretion ribonuclease used as a model for the potential involvement of mammalian RNases in the host defense system.[9,10] Expressed mainly in eosinophils and selectively released at the inflammation area,[11,12] ECP is reportedly involved in immunoregulation and tissue remodeling processes.[13,14] Its broad antibacterial spectrum includes both Gram-negative and -positive strains at a low micromolar range.[15] Although its mechanism of action is not completely understood, ECP has been described to act through a carpet-like mechanism, causing membrane destabilization and subsequent vesiculation.[16] ECP also has high affinity for bacterial cell wall components, such as lypopolysaccharide and peptidoglycans,[17] and a strong tendency to aggregate *Escherichia coli* cells.[18]

A previous attempt to delineate the antibacterial domain of ECP led to the identification of the N-terminus (residues 1−45) as the main antibacterial domain of the protein.[19] We have probed deeper into this region and in this paper describe how antimicrobially equipotent analogues of substantially reduced size (and consequently synthetic difficulty and costs) can be successfully derived from ECP by a structural minimization approach.

RESULTS AND DISCUSSION

Peptide Design and Synthesis. The starting point for a simplified ECP-derived antimicrobial lead candidate was the

Received: June 2, 2011

   dx.doi.org/10.1021/jm200701g | *J. Med. Chem.* XXXX, XXX, 000–000

Table 1. Sequence Information[a] and Chemical Properties of ECP Analogues

Peptide	ECP residues	Sequence	HPLC retention time (min)[b]	[M+H]$^+$ Theory	[M+H]$^+$ Found
		TT α1 α2 β1			
1	1-45	RPPQFTRAQWFAIQHISLNPPRSTIAMRAINNYRWRSKNQNTFLR	5.05 (20-40%)	5479.91	5483.50[c]
2	24-45	TIAMRAINNYRWRSKNQNTFLR	6.13 (10-45%)	2752.46	2753.28
3	1-19	RPPQFTRAQWFAIQHISLN	6.19 (15-50%)	2310.22	2311.73
4	8-45	AQWFAIQHISLNPPRSTIAMRAINNYRWRSKNQNTFLR	5.72 (15-60%)	4598.43	4598.88
5	8-36	AQWFAIQHISLNPPRSTIAMRAINNYRWR	6.66 (15-50%)	3509.85	3510.54
6	16-45	ISLNPPRSTIAMRAINNYRWRSKNQNTFLR	5.80 (10-60%)	3616.94	3617.87
7	(6-17)~(23-36)	TRAQWFAIQHIS-Ahx-STIAMRAINNYRWR	6.79 (10-60%)	3302.75	3303.29
8	(8-15)~(23-36)	AQWFAIQH--Ahx--STIAMRAINNYRWR	5.60 (15-60%)	2845.49	2845.26
9	(8-15)~(23-31)	AQWFAIQH--Ahx--STIAMRAIN	5.28 (15-60%)	2070.10	2070.00

[a] Secondary structure elements (based on ECP structure) shown above peptide **1** sequence. [b] In parentheses, linear gradient (solvent B into A over 15 min; see Experimental Section for details) used for optimal separation. [c] MALDI TOF mass spectrum acquired in the linear mode.

previously defined ECP N-terminal domain comprising the first 45 residues.[19] ECP(1−45) (**1**, Table 1) preserved the antimicrobial properties of native ECP, bound LPS with high affinity, and could permeabilize lipid vesicles at submicromolar concentration. Dissection of this domain into two peptides containing respectively the α1 and α2 helices, namely, ECP(1−19) and ECP(24−45) (**2**, **3**; Table 1), met with only partial success, as antimicrobial activity was substantially reduced in both analogues, particularly in **2**.[19] Recent NMR work on peptide **1**,[20] on the other hand, showed it to be partially unstructured in water and yet with two incipient α-helices closely matching α1 and α2 of native ECP, respectively, the latter expanding all the way down to the C-terminus of **1**. The α-helical trend was significantly enhanced in the presence of lipid vesicles, as is often the case. In light of these structural data, in our next attempt to define an ECP antimicrobial pharmacophore we have sought to keep together, albeit minimalistically, both α1 and α2 helical regions which, as usual in AMPs, are expected to be involved in membrane interaction. This hypothesis has led to a new set of analogues (**4**−**9**, Table 1) displaying various levels of ECP(1−45) sequence coverage and allowing outlining of a substantially simplified pharmacophore.

Three of the six new analogues entail various levels of trimming of the **1** sequence (Table 1), from moderate (**4**, first 7 N-terminal residues) to more drastic (**5**, first 7 N-terminal plus nine C-terminal; **6**, first 15 N-terminal residues), but all maintaining both α1 and α2 helical segments and an unsplit (internal) sequence. For the other three analogues (**7**−**9**), even more reductionistic criteria were applied, namely, dissecting out the 5−7 intervening loop residues (ISLNPPR) between α1 and α2 and replacing them by a flexible 6-aminohexanoic acid (Ahx) connector, an approach proven successful in linking discontinuous bioactive segments of polypeptide neurotransmitters.[21,22]

All analogues were successfully prepared by Fmoc-based, solid phase peptide synthesis protocols,[23] purified to homogeneity by HPLC, and identified by MALDI-TOF mass spectrometry. As in our earlier ECP dissection exercise,[19] the Cys23 and Cys37 residues, disulfide-bonded respectively to Cys83 and Cys96 and keeping the N-terminus tied to the rest of the ECP structure, were mutated to Ser in all analogues to prevent formation of unwanted intra- or intermolecular disulfide-linked species.

Activity and Structure of ECP Analogues. The six new analogues (**4**−**9**) were tested for antimicrobial activity against three Gram-negative and three Gram-positive species (Table 2). As a broader panel of bacteria than in a previous study[19] was available, both ECP and ECP(1−45) (**1**), the latter closely matching the former in antimicrobial spectrum,[19] were retested as reference compounds, as were single-helix analogues **2** and **3**. Antimicrobial profiles were complemented by a hemolysis assay (Table 2) as a measure of toxicity toward eukaryotic cells and by CD spectroscopy to evaluate peptide structure in the presence of either SDS or bacterial lipopolysaccharide (LPS) (Figure 1, Table 3), two micelle-promoting, membrane-like environments, the latter being the fundamental component of the Gram-negative bacterial cell wall. In addition, assays for liposome leakage, LPS binding, and *E. coli* agglutination (Table 4) were performed, the last two regarded as descriptive parameters of AMP activity against Gram-negative bacteria.[17] The goal of such an exhaustive comparison on both bacterial and artificial membrane systems was to outline the minimal sequence conferring antimicrobial properties to native ECP.

For analogues **1**−**3**, the above assays corroborated previous data,[19] namely, (i) the practical equipotency of **1** and native ECP on a representative set of bacteria, with a certain preference for Gram-negatives and MIC values slightly in the submicromolar range, the only exception being *M. luteus* (Table 2), (ii) the decrease (1 log unit on average) of antimicrobial activity in **2** and its virtually complete loss in analogue **3**, indicative of the crucial role of both the α2 and α1 helical segments, especially the former one, (iii) a slight increase in hemolytic activity of peptides **1**−**3** relative to the native protein (Table 2), and (iv) a correlation between the level of peptide structuration (representative CD spectra in Table 3), on the one hand, and membrane lytic and LPS binding activities (Table 4).

Among the six new analogues, the first three (**4**−**6**) displayed various levels of sequence shortening at the N- or C-terminus or

dx.doi.org/10.1021/jm200701g |J. Med. Chem. XXXX, XXX, 000–000

Table 2. Bactericidal (MIC_{100} in μM) and Hemolytic Activity (HC_{50} in μM) of ECP and Analogues

		bactericidal activity						
peptide	size reduction vs **1** (%)	*Escherichia coli*	*Pseudomonas* sp.	*Acinetobacter baumannii*	*Staphylococcus aureus*	*Micrococcus luteus*	*Enterococcus faecium*	hemolytic activity
ECP		0.4 ± 0.1	0.62 ± 0.07	0.6 ± 0.1	0.40 ± 0.06	1.5 ± 0.3	0.87 ± 0.07	>25
1	100	0.62 ± 0.07	0.6 ± 0.1	0.6 ± 0.1	0.62 ± 0.07	1.5 ± 0.3	0.87 ± 0.07	11.7 ± 0.2
2	51	7 ± 1	7 ± 1	1.1 ± 0.2	1.5 ± 0.3	7 ± 1	7 ± 1	18.7 ± 0.1
3	48	>10	>10	>10	>10	>10	>10	11.2 ± 0.1
4	16	0.45 ± 0.09	1.5 ± 0.3	0.88 ± 0.07	0.7 ± 0.1	1.5 ± 0.3	1.5 ± 0.3	10.5 ± 0.2
5	36	1.5 ± 0.3	3.5 ± 0.9	1.5 ± 0.3	0.7 ± 0.1	3.5 ± 0.9	1.5 ± 0.3	10.3 ± 0.1
6	33	1.5 ± 0.3	1.5 ± 0.3	3.5 ± 0.9	1.5 ± 0.3	3.5 ± 0.9	3.5 ± 0.9	10.5 ± 0.2
7	40	0.6 ± 0.1	1.5 ± 0.3	0.88 ± 0.07	0.87 ± 0.07	1.5 ± 0.3	1.5 ± 0.3	7.3 ± 0.1
8	49	1.5 ± 0.3	3.5 ± 0.9	7 ± 1	1.1 ± 0.2	>10	>10	14.4 ± 0.1
9	60	>10	>10	>10	>10	>10	>10	15.2 ± 0.1
CA(1−8)M(1−18)		1.1 ± 0.2	0.6 ± 0.1	0.88 ± 0.07	0.4 ± 0.1	1.5 ± 0.3	1.5 ± 0.3	7.8 ± 0.2

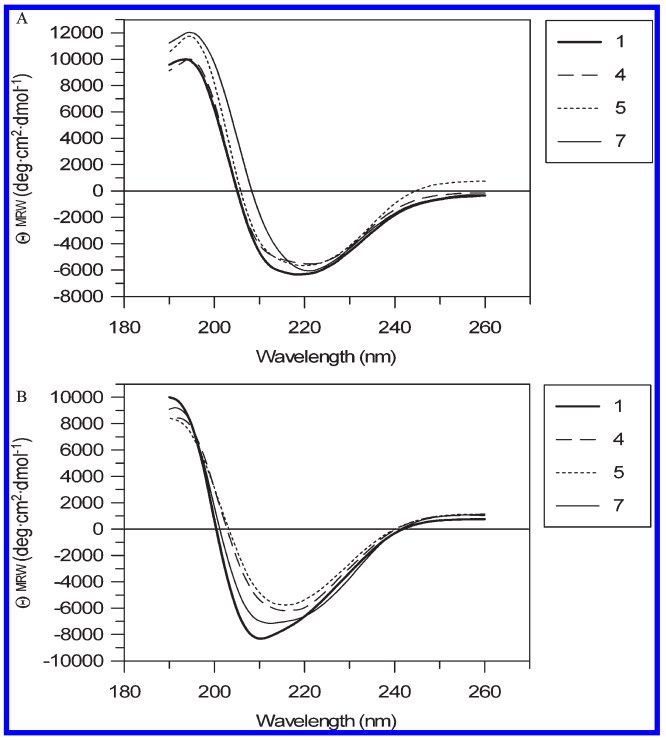

Figure 1. CD spectra of representative peptides in the presence of SDS (A) and LPS (B) micelles, as described in the Experimental Section.

both, in all cases less drastic (16−36% size reduction vs **1**) than **2** or **3** above but nonetheless quite informative. Thus, N-terminally truncated **4** underwent a minor loss in antimicrobial activity with respect to **1** (Table 2) while maintaining comparable levels of α-helix structure in the presence of SDS and LPS micelles (Figure 1, Table 3) as well as similar liposome leakage activities (Table 4). The lower affinity of **4** for LPS (ED_{50} of 1.58 vs 0.78 μM for **1**) appeared consistent with its reduced though still significant *E. coli* agglutination activity. Further trimming of **4** at the C-terminus, as in analogue **5**, entailed a loss in activity, mainly (2- to 5-fold vs **1**) against Gram-negatives and less pronounced against Gram-positives (Table 2). This loss of activity correlated with a decrease in both liposome leakage and LPS binding abilities

Table 3. α-Helix Content (in %) in the Presence of SDS and LPS Micelles As Determined by CD

peptide	SDS	LPS
1	73.1	35.9
2	60.8	16.8
3	68.4	3.8
4	69.1	27.8
5	69.1	26.4
6	64.2	15.2
7	73.0	35.5
8	55.3	29.5
9	60.7	29.7

Table 4. Liposome Leakage, LPS Binding, and *E. coli* Agglutination of Analogues 1−9

	ED_{50} (μM)		
peptide	liposome leakage	LPS binding	*E. coli* agglutination
1	0.41 ± 0.06	0.78 ± 0.05	++[b]
2	1.25 ± 0.06	1.52 ± 0.03	−
3	ND[a]	ND[a]	−
4	0.40 ± 0.05	1.58 ± 0.06	+[c]
5	0.74 ± 0.07	2.43 ± 0.05	+[c]
6	0.76 ± 0.10	6.13 ± 0.09	−
7	0.82 ± 0.10	1.60 ± 0.08	+[c]
8	1.63 ± 0.09	1.95 ± 0.03	−
9	ND[a]	5.13 ± 0.09	−

[a] No activity detected below 10 μM peptide concentration. [b] Minimal agglutinating concentration (MAC) below 0.5 μM. [c] MAC below 1 μM.

(Table 4), while in contrast the α-helical content of the peptide in the presence of SDS and LPS micelles was practically indistinguishable from that found for **4**. However, further truncation of **4** by eight extra residues at the N-terminus to give the analogue **6** not only caused a general deterioration of the antimicrobial profile relative to **4** (Table 2) but also diminished structuration in micelle environment (particularly LPS), a sharp loss in LPS binding ability, and the practical disappearance of agglutination

dx.doi.org/10.1021/jm200701g |J. Med. Chem. XXXX, XXX, 000–000

ability (Table 4). This last deficiency is consistent with the fact that, in contrast to **4** and **5**, analogue **6** lacks the region (residues 8−16) with the highest aggregation potential, as predicted by the Aggrescan[24] software and confirmed by site-directed mutagenesis,[25] while analogues **4** and **5** retain such a region and also show significant agglutinating behavior. Further comparative insights into the binding of the peptides may be obtained by the shifts observed in Trp fluorescence upon binding to liposomes or bacterial wall components such as LPS and lipoteichoic acid (LTA). Thus, analogues **4**−**6** displayed substantial red shifts in front of lipid vesicles (Table S1, Supporting Information), while in LPS and LTA environments, significant shifts were observed, respectively, for **4** and **5** and for **4** alone. Therefore, LTA binding would not seem to correlate with antimicrobial activity on Gram-positive strains for these peptides, whereas a good correlation between LPS binding and antimicrobial activity can be drawn for the Gram-negative strains.

Taking then peptide **5** as the smallest analogue retaining most of the antimicrobial activity, we attempted a more radical minimization that might eventually allow the outlining of an antimicrobial pharmacophore. To this end, a single spacer residue of recognized flexibility (6-aminohexanoic acid, Ahx)[22] was used to replace the loop connecting the α1 and α2 helices, with three new analogues (**7**−**9**) being designed and tested on such basis. Remarkably, the antimicrobial profile of analogue **7** not just preserved (Table 2) but indeed distinctly enhanced that of **5** against 4 out of the 6 test organisms. The superior performance was supported by findings such as an LPS binding capacity in the same range compared with much larger analogue **2** or **4** or an agglutinating ability parallel to **4** and **5** (Table 4) and was also fully consistent with structural data from CD, indicating an α-helix content similar to that of peptide **5** in both SDS and LPS micelles (Table 3) and especially with NMR data showing a remarkable preservation of native structure (see below).

Attempts at further size reduction by removal of two residues at each end of the N-terminal α1 helix to give analogue **8** met with a clear deterioration in antimicrobial properties, e.g., inactivity toward two of the Gram-positive test organisms as well as an abrupt drop in the activity against *Acinetobacter*. In tune with this, liposome leakage activity of **8** was about 2-fold reduced relative to any of the previous analogues, and its *E. coli* agglutinating ability was again lost, as also found for the poorly performing analogue **5** above. All these observations underscore the important contribution of the four removed residues, particularly of Arg7, recently shown to be involved in the binding of ECP to heparin and glycosaminoglycan structures,[20] an ability that might be similarly relevant in the interaction with the Gram-negative bacteria cell wall. Finally, the attempt to dispense with the α2 helix at the C-terminal section led to an analogue (**9**) totally unable to cause microbial cell death below 10 μM (Table 2). These adverse results correlated rather well with the substantial loss in helical structure for both **8** and **9** (Table 3), with their pronounced decrease in LPS binding (Table 4), or with the smaller red shifts in Trp fluorescence found for **8** upon incubation with LTA or for **9** with both LPS and LTA (Table S1, Supporting Information), the latter suggesting that binding to the cell wall envelope is determinant in the antimicrobial action of these peptides. The inactivity of analogue **9**, C-terminally truncated from residue 31 onward, is expected on the basis of a sequence scanning algorithm[26] that predicts for positions downstream from Ile30, an antimicrobial region that would logically be missing in **9**. Equally or more eloquent for the inactivity of **9** are structural factors such as the absence of Trp35, a residue known to be required for membrane binding and lysis,[16] or the similar lack of Arg36, which together with Trp35 has been related to glycosaminoglycan binding in biophysical studies[17,18,27] and to antimicrobial activity in mutagenesis studies.[15,28] Also, a chimera recently constructed by inserting the ECP(33−36) sequence (which **9** lacks) into a nontoxic RNase was shown to endow it with some bactericidal activity.[29]

NMR Solution Structure of Analogue 7. Further support for the suitability of analogue **7** was obtained from NMR structural studies. Although the ^{1}H NMR spectra of **7** in aqueous solution (pH 4.4, 25 °C) showed limited chemical shift dispersion, indicating that no preferred stable secondary structure was adopted, analysis of the conformational shifts ($\Delta\delta_{H\alpha}$) showed some helical tendency between Ala8-Gln14 and Ile25-Arg36, with ∼28% and ∼24% helix populations in these segments estimated from the chemical shift data,[33] respectively. In dodecylphosphocoline (DPC) micelles the spectra showed more disperse chemical shifts compared to the water solution (Table S2, Supporting Information), allowing for helical regions at each end of the Ahx linker to be clearly delineated: an N-terminal segment spanning Arg7-His15 (population 51%) and a C-terminal segment spanning Ser23-Arg36 (population 64%).

As is often the case with isolated peptides, conformational equilibria preclude the interpretation of the NMR data of **7** in terms of a single structure. Nonetheless, calculation of a limited number of structures compatible with the experimental data is a general and useful way to visualize the structural features of the favored family of structures present in the conformational ensemble of the peptide. Such a model structure is shown in Figure 2A for analogue **7** in DPC micelles. The calculations were done as described in Experimental Section, and statistics are summarized in Table S3, Supporting Information. The model structures are quite well-defined within the helical peptide segments previously determined on the basis of $\Delta\delta_{H\alpha}$. The N-terminal α-helical stretch approximately coincides with that previously reported for the native α_1 helix of ECP (Arg7-Ile16)[34] and **1**,[20] and the C-terminal α-helical stretch similarly matches the native α_2 helix of ECP (Cys23-Asn31)[34] (Figure 2B). While the Ahx residue is too flexible to induce a preferred relative orientation of both helical regions and thus a clear-cut segregation of polar/hydrophobic residues, it is interesting that in most conformers residues Trp10 and Ile13 of the N-terminal and Ile30 and Tyr33 of the C-terminal helices are oriented toward the concave face of the structure, in a disposition similar to that adopted by these side chains in the native ECP structure.

Final Remarks. In this work we have shown how structure-guided minimization of the ECP(1−45) antimicrobial domain leads to analogues such as **4**−**7**, with substantial size reduction [for **7**, 40% vs ECP(1−45) or 80% vs native ECP] and yet displaying a broad, potent antimicrobial spectrum not dissimilar to that of either ECP(1−45) or native ECP. On the basis of the present data, analogue **7** displays an optimal balance between antimicrobial efficacy and structural simplicity, and the NMR evidence that it preserves to a substantial degree the α-helical features of ECP confirms our previous proposal[34,20] of the α1 and α2 helices as the antimicrobially relevant pharmacophore of ECP and hence a useful template for the development of ECP-based AMPs. A slight increase in hemolytic activity of **7** (HC_{50} = 7.3 ± 0.1 μM) relative to other analogues (HC_{50} ≈ 10 μM, Table 2) is of minor concern; indeed, **7** parallels in both antimicrobial and hemolytic activity as well as in size, a recognized

dx.doi.org/10.1021/jm200701g |J. Med. Chem. XXXX, XXX, 000–000

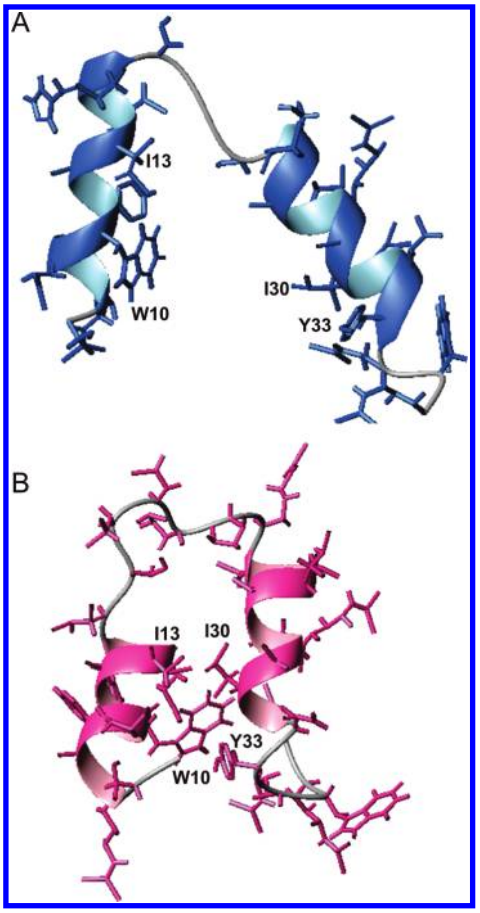

Figure 2. (A) Molecular model of peptide **7** as determined by NMR spectroscopy. (B) Helices α1 and α2 of native ECP (PDB code 2KB5). Residues W10, I13, I30, and Y33 pointing to the helical interface are labeled.

AMP standard such as the cecropin−melittin hybrid CA(1−8)-M(1−18) (Table 2).[30−32] In conclusion, our data allow us to propose **7** as an ideally downsized version of ECP and hence a valuable antimicrobial lead structure.

EXPERIMENTAL SECTION

Materials. DOPC (dioleoyl phosphatidylcholine) and DOPG (dioleoyl phosphatidylglycerol) were from Avanti Polar Lipids (Alabaster, AL). ANTS (8-aminonaphthalene-1,3,6-trisulfonic acid disodium salt), DPX (*p*-xylenebispyridinium bromide), and BC (BODIPY TR cadaverine, where BODIPY is boron dipyrromethane (4,4-difluoro-4-bora-3a,4a-diaza-*s*-indacene) were purchased from Invitrogen (Carlsbad, CA). LT (lipoteichoic acids) from *Staphylococcus aureus* and LPS (lipopolysaccharides) from *Eschericha coli* serotype 0111:B4 were purchased from Sigma-Aldrich (St. Louis, MO). PD-10 desalting columns with Sephadex G-25 were from GE Healthcare (Waukesha, WI). Strains used were *Escherichia coli* (BL2, Novagen), *Staphylococcus aureus* (ATCC 502A), *Acinetobacter baumannii* (ATCC 15308), *Pseudomonas sp* (ATCC 15915), *Micrococcus luteus* (ATCC 7468), and *Enterococcus faecium* (ATCC 19434).

Peptides. Fmoc-protected amino acids and 2-(1*H*-benzotriazol-1-yl)-1,1,3,3-tetramethyluronium hexafluorophosphate (HBTU) were obtained from Iris Biotech (Marktredwitz, Germany). Fmoc-Rink-amide (MBHA) resin was from Novabiochem (Laüfelfingen, Switzerland). HPLC-grade acetonitrile (ACN) and peptide synthesis-grade *N*, *N*-dimethylformamide (DMF), *N*,*N*-diisopropylethylamine (DIEA), and trifluoroacetic acid (TFA) were from Carlo Erba-SDS (Peypin, France).

Solid phase peptide synthesis was done by Fmoc-based chemistry on Fmoc-Rink-amide (MBHA) resin (0.1 mmol) in a model 433 synthesizer (Applied Biosystems, Foster City, CA) running FastMoc protocols. Couplings used 8-fold molar excess each of Fmoc-amino acid and HBTU and 16-fold molar excess of DIEA. Side chains of trifunctional residues were protected with *tert*-butyl (Ser, Thr, Tyr), *tert*-butyolxycarbonyl (Lys, Trp), 2,2,4,6,7-pentamethyldihydrobenzofuran-5-sulfonyl (Arg), and trityl (Asn, Gln, His) groups. After chain assembly, full deprotection and cleavage were carried out with TFA−water−triisopropylsilane (95:2.5:2.5 v/v, 90 min, room temperature). Peptides were isolated by precipitation with cold diethyl ether and separated by centrifugation, dissolved in 0.1 M acetic acid, and lyophilized. Analytical reversed-phase HPLC was performed on a Luna C_{18} column (4.6 mm × 50 mm, 3 μm; Phenomenex, CA). Linear gradients of solvent B (0.036% TFA in ACN) into A (0.045% TFA in H_2O) were used for elution at a flow rate of 1 mL/min and with UV detection at 220 nm. Preparative HPLC runs were performed on a Luna C_{18} column (21.2 mm × 250 mm, 10 μm; Phenomenex, CA), using linear gradients of solvent B (0.1% in ACN) into A (0.1% TFA in H_2O), as required, with a flow rate of 25 mL/min. MALDI-TOF mass spectra were recorded in the reflector or linear mode in a Voyager DE-STR workstation (Applied Biosystems, Foster City, CA) using α-hydroxycinnamic acid matrix. Fractions of adequate (>90%) HPLC homogeneity and with the expected mass were pooled, lyophilized, and used in subsequent experiments.

Expression and Purification of ECP. Wild-type ECP was obtained from a human ECP synthetic gene. Protein expression in the *E. coli* BL21DE3 strain, folding of the protein from inclusion bodies, and purification were carried out as previously described.[35]

MIC (Minimal Inhibitory Concentration) Determination. Antimicrobial activity was expressed as the MIC, defined as the lowest peptide concentration that completely inhibits microbial growth. MIC of each peptide was determined from two independent experiments performed in triplicate for each concentration. Peptides were dissolved in 10 mM sodium phosphate buffer, pH 7.5, and serially diluted from 10 to 0.2 μM. Bacteria were incubated at 37 °C overnight in Luria−Bertani broth and diluted to give approximately 5×10^5 CFU/mL. In each assay peptide solutions were added to each bacteria dilution and incubated for 4 h, and samples were plated onto Petri dishes and incubated at 37 °C overnight.

Minimal Agglutination Activity. *E. coli* cells were grown at 37 °C to mid-exponential phase (OD_{600} = 0.6), centrifuged at 5000*g* for 2 min, and resuspended in Tris-HCl buffer, 0.15 M NaCl, pH 7.5, in order to give an absorbance of 10 at 600 nm. A 200 μL aliquot of the bacterial suspension was incubated with peptide at various (0.1−10 μM) concentrations at 25 °C overnight. Aggregation behavior was observed by visual inspection and minimal agglutinating concentration expressed as previously described[36]

Hemolytic Activity. Fresh human red blood cells (RBCs) were washed 3 times with PBS (35 mM phosphate buffer, 0.15 M NaCl, pH 7.4) by centrifugation for 5 min at 3000*g* and resuspended in PBS at 2×10^7 cells/mL. RBCs were incubated with peptides at 37 °C for 4 h and centrifuged at 13000*g* for 5 min. The supernatant was separated from the pellet and its absorbance measured at 570 nm. The 100% hemolysis was defined as the absorbance obtained by sonicating RBCs for 10 s. HC_{50} was calculated by fitting the data to a sigmoidal function.

Liposome Preparation. LUVs (large unilamellar vesicles) of ∼100 nm diameter were prepared from a chloroform solution of DOPC/DOPG (3:2 molar ratio). After vacuum-drying, the lipid film was suspended in 10 mM Tris/HCl, 0.1 M NaCl, pH 7.4 buffer to give a 1 mM solution, then frozen and thawed several times prior to extrusion through polycarbonate membranes as previously described.[18]

dx.doi.org/10.1021/jm200701g |*J. Med. Chem.* XXXX, XXX, 000–000

Fluorescence Measurements. Tryptophan fluorescence emission spectra were recorded using a 280 nm excitation wavelength. Slits were set at 2 nm for excitation and 5−10 nm for emission. Emission spectra were recorded from 300−400 nm at a scan rate of 60 nm/min in a 10 mm ×10 mm cuvette, with stirring immediately after sample mixing. Protein and peptide spectra at 0.5 μM in 10 mM Hepes buffer, pH 7.4, were obtained at 25 °C in the absence or presence of 200 μM liposome suspension, 200 μM LPS (assuming a 90 000 g/mol molecular mass), or 200 μM LTA, as calculated from a 2200 molecular mass reference value. Fluorescence measurements were performed on a Cary Eclipse spectrofluorimeter. Spectra in the presence of liposomes were corrected for light scattering by subtracting the corresponding LUV background. For each condition three spectra were averaged. The fluorescence spectra were also calculated as a function of the frequency scale (wavenumber) and adjusted using a log normal function as detailed previously.[16]

LPS Binding Assay. LPS binding was assessed using the fluorescent probe Bodipy TR cadaverine (BC) as described.[17] Briefly, the displacement assay was performed by the addition of 1−2 μL aliquots of ECP or peptide solution to 1 mL of a continuously stirred mixture of LPS (10 μg·mL^{-1}) and BC (10 μm) in 5 mm Hepes buffer at pH 7.5. Fluorescence measurements were performed on a Cary Eclipse spectrofluorimeter. The BC excitation wavelength was 580 nm, and the emission wavelength was 620 nm. The excitation slit was set at 2.5 nm, and the emission slit was set at 20 nm. Final values correspond to an average of four replicates and were the mean of a 0.3 s continuous measurement. Quantitative effective displacement values (ED_{50}) were calculated.

ANTS/DPX Liposome Leakage Assay. The ANTS/DPX liposome leakage fluorescence assay was performed as described.[18] Briefly, a unique population of LUVs of DOPC/DOPG (3:2 molar ratio) lipids was obtained containing 12.5 mM ANTS, 45 mM DPX, 20 mM NaCl, and 10 mM Tris/HCl, pH 7.5. The ANTS/DPX liposome suspension was diluted to 30 μM and incubated at 25 °C in the presence of ECP or peptides. The percentage of leakage (%L) was determined by monitoring the release of liposome content at peptide concentrations up to 10 μM after 1 h of incubation, as follows: $\%L = 100(F_p - F_0)/(F_{100} - F_0)$, where F_p is the final fluorescence intensity after peptide addition (1 h) and F_0 and F_{100} are the fluorescence intensities before peptide addition and after addition of 0.5% Triton X100. ED_{50} was calculated by fitting the data to a sigmoidal function.

CD Spectroscopy. Far-UV CD spectra were obtained from a Jasco J-715 spectropolarimeter as described.[19] Mean-residue ellipticity $[\theta]$ (deg·cm^2·dmol^{-1}) was calculated as

$$[\theta] = \frac{\theta(\mathrm{MRW})}{10cl}$$

where θ is the experimental ellipticity (deg), MRW is the mean residue molecular mass of the peptide, c is the molar concentration of peptide, and l is the cell path length. Data from four consecutive scans were averaged. Spectra of ECP and peptides (4−8 μM in 5 mM sodium phosphate, pH 7.5) in the absence and presence (1 mM) of SDS and LPS (1 mM, nominal MW = 90 kDa) were recorded. Samples were centrifuged for 5 min at 10000g before use. Percentage of secondary structure was estimated with the Jasco software, as described by Yang et al.[37] and by the Selcon software.[38]

NMR Spectroscopy. Peptide **7** samples for NMR were prepared at ∼1 mM in 90% H_2O/10% D_2O or ∼50 mM [$^2H_{38}$]dodecylphosphocholine (DPC, Cambridge Isotope Laboratories) in 90% H_2O/10% D_2O. The pH was adjusted to 4.4 at 25 °C with no correction for isotope effects. NMR experiments were performed in a Bruker AV-800 instrument equipped with a cryoprobe and field gradients. All data were acquired and processed with TOPSPIN (version 1.3) (Bruker, Germany) at two temperatures, 25 and 35 °C. COSY, TOCSY, NOESY, and $^1H-^{13}C$ HSQC spectra were acquired with standard pulse sequences. Water suppression was accomplished with presaturation or by using the WATERGATE module.[39] Mixing times were 60 and 150 ms for the TOCSY and NOESY experiments, respectively. The spectral assignment of the peptide in the different solvents was performed by following the well-established sequential-specific methodology based on homonuclear spectra.[40]

Helix population in the peptide segments was quantified from $^1H_\alpha$ conformational chemical shift values, $\Delta\delta_{H\alpha}$.[33] To obtain the helix percentage, the $\Delta\delta_{H\alpha}\Delta\delta_{H\alpha} = \delta_{H\alpha}^{\text{observed}} - \delta_{H\alpha}^{\text{random coil}}$ values for all the residues were averaged, divided by the $\Delta\delta_{H\alpha}$ value corresponding to 100% helix, −0.39 ppm,[41] and multiplied by 100. The random coil values were from Wishart et al.[42]

The 3D structure of the peptide in DPC was obtained from distance constraints derived from a NOESY spectrum at 25 °C with 150 ms mixing time. The NOE cross-peaks were integrated with the automatic subroutine of the SPARKY program[43] and then calibrated and converted into upper limit distance constraints. Structures were calculated using the CYANA (version 2.1) program[44] with the distance constraints and backbone dihedral angle ranges obtained from TALOS.[45] Finally, the structures were energy-minimized and refined. Families of 50 structures satisfactorily reproducing the experimental constraints were generated; the best 20 of such structures on the basis of energies and Ramachandran plot quality were selected for further analysis. All structures were visualized and analyzed with MOLMOL.[46]

■ ASSOCIATED CONTENT

Ⓢ Supporting Information. Characterization of the peptide tryptophan spectra in the presence of lipid vesicles, LPS micelles, and LTA micelles; HN and Hα chemical shifts of analogue **7** in water and DPC micelles; statistics of structural restraints and violations. This material is available free of charge via the Internet at http://pubs.acs.org.

■ AUTHOR INFORMATION

Corresponding Author

*For D.A.: phone, +34-933160868; fax, +34-933161901; e-mail, david.andreu@upf.edu. For E.B.: phone, +34- 935814147; e-mail, ester.boix@uab.cat.

■ ACKNOWLEDGMENT

M.T. is a recipient of an Alianza Cuatro Universidades fellowship. Work was supported by the Spanish Ministry of Science and Innovation [Grants BFU2009-09371 to E.B., BIO2008-04487-CO3-02 to D.A., and CTQ2008-00080 to M.B.], Generalitat of Catalonia [Grants SGR2009-795 and SGR2009-494], and the European Union [Grant HEALTH-F3-2008-223414 (LEISHDRUG) to D.A.].

■ ABBREVIATIONS USED

Ahx, aminohexanoic acid; AMP, antimicrobial peptide; COSY, correlation spectroscopy; DOPC, dioleoyl phosphatidylcholine; DOPG, dioleoyl phosphatidylglycerol; DPC, [$^2H_{38}$]dodecylphosphocholine; ECP, eosinophil cationic protein; HSQC, heteronuclear single quantum coherence; LPS, lipopolysaccharide; LTA, lipoteichoic acid; LUV, large unilamellar vesicle; MIC, minimum inhibitory concentration; NOE, nuclear Overhauser effect; NOESY, nuclear Overhauser effect spectroscopy; SDS, sodium dodecyl sulfate; TOCSY, total correlation spectroscopy

REFERENCES

(1) Hadley, E. B.; Hancock, R. E. Strategies for the discovery and advancement of novel cationic antimicrobial peptides. *Curr. Top. Med. Chem.* **2010**, 1872–1881.

(2) Shai, Y. Mode of action of membrane active antimicrobial peptides. *Biopolymers* **2002**, *66*, 236–248.

(3) Yeaman, M. R.; Yount, N. Y. Mechanisms of antimicrobial peptide action and resistance. *Pharmacol. Rev.* **2003**, *55*, 27–55.

(4) Ramanathan, B.; Davis, E. G.; Ross, C. R.; Blecha, F. Cathelicidins: microbicidal activity, mechanisms of action, and roles in innate immunity. *Microbes Infect.* **2002**, *4*, 361–372.

(5) Rathinakumar, R.; Walkenhorst, W. F.; Wimley, W. C. Broad-spectrum antimicrobial peptides by rational combinatorial design and high-throughput screening: the importance of interfacial activity. *J. Am. Chem. Soc.* **2009**, *131*, 7609–7617.

(6) Romestand, B.; Molina, F.; Richard, V.; Roch, P.; Granier, C. Key role of the loop connecting the two beta strands of mussel defensin in its antimicrobial activity. *Eur. J. Biochem.* **2003**, *270*, 2805–2813.

(7) Vila-Perello, M.; Sanchez-Vallet, A.; Garcia-Olmedo, F.; Molina, A.; Andreu, D. Structural dissection of a highly knotted peptide reveals minimal motif with antimicrobial activity. *J. Biol. Chem.* **2005**, *280*, 1661–1668.

(8) Vila-Perello, M.; Tognon, S.; Sanchez-Vallet, A.; Garcia-Olmedo, F.; Molina, A.; Andreu, D. A minimalist design approach to antimicrobial agents based on a thionin template. *J. Med. Chem.* **2006**, *49*, 448–451.

(9) Cho, S.; Beintema, J. J.; Zhang, J. The ribonuclease A superfamily of mammals and birds: identifying new members and tracing evolutionary histories. *Genomics* **2005**, *85*, 208–220.

(10) Dyer, K. D.; Rosenberg, H. F. The RNase a superfamily: generation of diversity and innate host defense. *Mol. Diversity* **2006**, *10*, 585–597.

(11) Boix, E.; Nogues, M. V. Mammalian antimicrobial proteins and peptides: overview on the RNase A superfamily members involved in innate host defence. *Mol. BioSyst.* **2007**, *3*, 317–335.

(12) Boix, E.; Torrent, M.; Sanchez, D.; Nogues, M. V. The antipathogen activities of eosinophil cationic protein. *Curr. Pharm. Biotechnol.* **2008**, *9*, 141–152.

(13) Rubin, J.; Zagai, U.; Blom, K.; Trulson, A.; Engstrom, A.; Venge, P. The coding ECP 434(G>C) gene polymorphism determines the cytotoxicity of ECP but has minor effects on fibroblast-mediated gel contraction and no effect on RNase activity. *J. Immunol.* **2009**, *183*, 445–451.

(14) Zagai, U.; Skold, C. M.; Trulson, A.; Venge, P.; Lundahl, J. The effect of eosinophils on collagen gel contraction and implications for tissue remodelling. *Clin. Exp. Immunol.* **2004**, *135*, 427–433.

(15) Carreras, E.; Boix, E.; Rosenberg, H. F.; Cuchillo, C. M.; Nogues, M. V. Both aromatic and cationic residues contribute to the membrane-lytic and bactericidal activity of eosinophil cationic protein. *Biochemistry* **2003**, *42*, 6636–6644.

(16) Torrent, M.; Cuyas, E.; Carreras, E.; Navarro, S.; Lopez, O.; de la Maza, A.; Nogues, M. V.; Reshetnyak, Y. K.; Boix, E. Topography studies on the membrane interaction mechanism of the eosinophil cationic protein. *Biochemistry* **2007**, *46*, 720–733.

(17) Torrent, M.; Navarro, S.; Moussaoui, M.; Nogues, M. V.; Boix, E. Eosinophil cationic protein high-affinity binding to bacteria-wall lipopolysaccharides and peptidoglycans. *Biochemistry* **2008**, *47*, 3544–3555.

(18) Torrent, M.; Nogues, M. V.; Boix, E. Eosinophil cationic protein (ECP) can bind heparin and other glycosaminoglycans through its RNase active site. *J. Mol. Recognit.* **2011**, *24*, 90–100.

(19) Torrent, M.; de la Torre, B. G.; Nogues, V. M.; Andreu, D.; Boix, E. Bactericidal and membrane disruption activities of the eosinophil cationic protein are largely retained in an N-terminal fragment. *Biochem. J.* **2009**, *421*, 425–434.

(20) Garcia-Mayoral, M. F.; Moussaoui, M.; de la Torre, B. G.; Andreu, D.; Boix, E.; Nogues, M. V.; Rico, M.; Laurents, D. V.; Bruix, M. NMR structural determinants of eosinophil cationic protein binding to membrane and heparin mimetics. *Biophys. J.* **2010**, *98*, 2702–2711.

(21) Beck-Sickinger, A. G.; Grouzmann, E.; Hoffmann, E.; Gaida, W.; van Meir, E. G.; Waeber, B.; Jung, G. A novel cyclic analog of neuropeptide Y specific for the Y2 receptor. *Eur. J. Biochem.* **1992**, *206*, 957–964.

(22) Beck-Sickinger, A. G.; Jung, G. Structure−activity relationships of neuropeptide Y analogues with respect to Y1 and Y2 receptors. *Biopolymers* **1995**, *37*, 123–142.

(23) Fields, G. B.; Noble, R. L. Solid phase peptide synthesis utilizing 9-fluorenylmethoxycarbonyl amino acids. *Int. J. Pept. Protein Res.* **1990**, *35*, 161–214.

(24) Conchillo-Sole, O.; de Groot, N. S.; Aviles, F. X.; Vendrell, J.; Daura, X.; Ventura, S. AGGRESCAN: a server for the prediction and evaluation of "hot spots" of aggregation in polypeptides. *BMC Bioinf.* **2007**, *8*, 65.

(25) Torrent, M.; Odorizzi, F.; Nogues, M. V.; Boix, E. Eosinophil cationic protein aggregation: identification of an N-terminus amyloid prone region. *Biomacromolecules* **2010**, *11*, 1983–1990.

(26) Torrent, M.; Nogues, V. M.; Boix, E. A theoretical approach to spot active regions in antimicrobial proteins. *BMC Bioinf.* **2009**, *10*, 373.

(27) Fan, T. C.; Fang, S. L.; Hwang, C. S.; Hsu, C. Y.; Lu, X. A.; Hung, S. C.; Lin, S. C.; Chang, M. D. Characterization of molecular interactions between eosinophil cationic protein and heparin. *J. Biol. Chem.* **2008**, *283*, 25468–25474.

(28) Carreras, E.; Boix, E.; Navarro, S.; Rosenberg, H. F.; Cuchillo, C. M.; Nogues, M. V. Surface-exposed amino acids of eosinophil cationic protein play a critical role in the inhibition of mammalian cell proliferation. *Mol. Cell. Biochem.* **2005**, *272*, 1–7.

(29) Torrent, G.; Ribo, M.; Benito, A.; Vilanova, M. Bactericidal activity engineered on human pancreatic ribonuclease and onconase. *Mol. Pharmaceutics* **2009**, *6*, 531–542.

(30) Andreu, D.; Ubach, J.; Boman, A.; Wahlin, B.; Wade, D.; Merrifield, R. B.; Boman, H. G. Shortened cecropin A-melittin hybrids. Significant size reduction retains potent antibiotic activity. *FEBS Lett.* **1992**, *296*, 190–194.

(31) Piers, K. L.; Brown, M. H.; Hancock, R. E. Improvement of outer membrane-permeabilizing and lipopolysaccharide-binding activities of an antimicrobial cationic peptide by C-terminal modification. *Antimicrob. Agents Chemother.* **1994**, *38*, 2311–2316.

(32) Piers, K. L.; Hancock, R. E. The interaction of a recombinant cecropin/melittin hybrid peptide with the outer membrane of *Pseudomonas aeruginosa*. *Mol. Microbiol.* **1994**, *12*, 951–958.

(33) Jimenez, M. A.; Bruix, M.; Gonzalez, C.; Blanco, F. J.; Nieto, J. L.; Herranz, J.; Rico, M. CD and ^{1}H-NMR studies on the conformational properties of peptide fragments from the C-terminal domain of thermolysin. *Eur. J. Biochem.* **1993**, *211*, 569–581.

(34) Laurents, D. V.; Bruix, M.; Jimenez, M. A.; Santoro, J.; Boix, E.; Moussaoui, M.; Nogues, M. V.; Rico, M. The ^{1}H, ^{13}C, ^{15}N resonance assignment, solution structure, and residue level stability of eosinophil cationic protein/RNase 3 determined by NMR spectroscopy. *Biopolymers* **2009**, *91*, 1018–1028.

(35) Boix, E.; Nikolovski, Z.; Moiseyev, G. P.; Rosenberg, H. F.; Cuchillo, C. M.; Nogues, M. V. Kinetic and product distribution analysis of human eosinophil cationic protein indicates a subsite arrangement that favors exonuclease-type activity. *J. Biol. Chem.* **1999**, *274*, 15605–15614.

(36) Torrent, M.; Badia, M.; Moussaoui, M.; Sanchez, D.; Nogues, M. V.; Boix, E. Comparison of human RNase 3 and RNase 7 bactericidal action at the Gram-negative and Gram-positive bacterial cell wall. *FEBS J.* **2010**, *277*, 1713–1725.

(37) Yang, J. T.; Wu, C. S.; Martinez, H. M. Calculation of protein conformation from circular dichroism. *Methods Enzymol.* **1986**, *130*, 208–269.

(38) Sreerama, N.; Woody, R. W. A self-consistent method for the analysis of protein secondary structure from circular dichroism. *Anal. Biochem.* **1993**, *209*, 32–44.

(39) Piotto, M.; Saudek, V.; Sklenar, V. Gradient-tailored excitation for single-quantum NMR spectroscopy of aqueous solutions. *J. Biomol. NMR* **1992**, *2*, 661–665.

(40) Wüthrich, K. *NMR of Proteins and Nucleic Acids*; Wiley-Interscience: New York, 1986.
(41) Wishart, D. S.; Sykes, B. D.; Richards, F. M. Relationship between nuclear magnetic resonance chemical shift and protein secondary structure. *J. Mol. Biol.* **1991**, *222*, 311–333.
(42) Wishart, D. S.; Bigam, C. G.; Holm, A.; Hodges, R. S.; Sykes, B. D. ^{1}H, ^{13}C and ^{15}N random coil NMR chemical shifts of the common amino acids. I. Investigations of nearest-neighbor effects. *J. Biomol. NMR* **1995**, *5*, 67–81.
(43) Goddard, T. D.; Kneller, D. G. *SPARKY*, version 3; University of California: San Francisco, CA, 2005.
(44) Guntert, P. Automated NMR structure calculation with CYANA. *Methods Mol. Biol.* **2004**, *278*, 353–378.
(45) Cornilescu, G.; Delaglio, F.; Bax, A. Protein backbone angle restraints from searching a database for chemical shift and sequence homology. *J. Biomol. NMR* **1999**, *13*, 289–302.
(46) Koradi, R.; Billeter, M.; Wuthrich, K. MOLMOL: a program for display and analysis of macromolecular structures. *J. Mol. Graphics* **1996**, *14* (51−55), 29–32.